Plant Reproduction (2019) 32:217–228
https://doi.org/10.1007/s00497-019-00368-7

ORIGINAL ARTICLE

A missense mutation of *STERILE APETALA* leads to female sterility in Chinese cabbage (*Brassica campestris* ssp. *pekinensis*)

Wenjie Liu[1] · Shengnan Huang[1] · Zhiyong Liu[1] · Tengxue Lou[2] · Chong Tan[1] · Yiheng Wang[1] · Hui Feng[1]

Received: 13 September 2018 / Accepted: 18 February 2019 / Published online: 26 February 2019

Abstract

Flower development is essential for the sexual reproduction and crop yield of plants. Thus, a better understanding of plant sterility from the perspective of morphological and molecular genetics is imperative. In our previous study, a recessive female-sterile Chinese cabbage mutant *fsm* was obtained from a doubled haploid line 'FT' via an isolated microspore culture combined with EMS mutagenesis. Pistil aniline blue staining and stigma scanning observation showed that the growth of the stigma papillar cells and pollen tubes of the mutant *fsm* were normal. Therefore, the female sterility was due to abnormal development of the ovules. To map the mutant *fsm*, 3108 F_2 individuals were selected for linkage analysis. Two closely linked markers, Indel-I2 and Indel-I7, were localized on the flanking region of *fsm* at distances of 0.05 cM and 0.06 cM, respectively. The physical distance between Indel-I2 and Indel-I7 was ~ 1376 kb, with 107 genes remaining in the target region. This region was located on the chromosome A04 centromere, on which low recombination rates and a high frequency of repetitive sequences were present. Whole-genome re-sequencing detected a single-nucleotide (C-to-A) transition (TCG/TAG) on the exon of *BraA04001030*, resulting in a premature stop codon. Genotyping revealed that the female-sterile phenotype was fully cosegregated with this SNP. *BraA04001030* encodes a homologue of *STERILE APETALA* (*SAP*) transcriptional regulator, which plays vital roles in floral development. The results of the present study suggest that *BraA04001030* is a strong candidate gene for *fsm* and provide the basis for exploring the molecular mechanism underlying female sterility in Chinese cabbage.

Keywords Chinese cabbage · EMS mutagenesis · Female-sterile · *STERILE APETALA*

Introduction

Flowering is the most significant feature of angiosperms. In this process, plants are transformed from vegetative to reproductive growth. Life cycle alternation between the diploid and haploid phases is complete in flower organs when the gametophyte is fertilized and becomes a sporophyte. In general, flowers are composed of four types of organs: sepals, petals, stamens, and carpels. The morphology of these structures may vary among species, but most carpels consist of a stigma, a style, and an ovary containing ovules (Kuusk et al. 2002). Historically, plant male sterility has been the focus of plant breeders. However, with the development of biotechnology, female sterility has been attracting increasing attention. Female sterility is classified into three main categories: (a) flowers with incomplete or no female organs; (b) flowers with abnormal ovule development or no megasporocytes; and (c) flowers with normal ovules that fail to develop into mature seeds after pollination (Li et al. 2006). The sterile phenotype might be attributed to changes to the sporophyte or gametophyte. Female-sterile mutants with malformed ovaries, ovules, embryo sacs, or megaspore mother cells have been induced using various molecular biology techniques (Sundaresan and Alandetesaez 2010; Yang et al. 2016; Liu et al. 2017; Cao et al. 2018). Female

Wenjie Liu and Shengnan Huang have contributed equally to this work and share the first authorship.

Electronic supplementary material The online version of this article (https://doi.org/10.1007/s00497-019-00368-7) contains supplementary material, which is available to authorized users.

✉ Hui Feng
fenghuiaaa@263.net

[1] Department of Horticulture, Shenyang Agricultural University, 120 Dongling Road, Shenhe District, Shenyang 110866, People's Republic of China

[2] Key Laboratory of Plant Molecular Physiology, Institute of Botany, Chinese Academy of Sciences, Beijing 100093, People's Republic of China

sterility facilitates the investigation of pistil and ovule development and the mechanisms underlying their genetic regulation (Bencivenga et al. 2011; Tedder et al. 2015; Wei et al. 2015; Zhou et al. 2016; Singh et al. 2017).

The pistil is located in the innermost floral whorl. It generates the embryo sac, functional megaspores, and mature seeds. The traditional ABC model of flower development classified several major function class genes that are specifically identified in each whorl. C-class genes alone control the carpels (Coen and Meyerowitz 1991; Pinyopich et al. 2003). High-throughput sequencing and molecular biology have identified many important genes in female-sterile mutants of *Arabidopsis* and other species (Tedder et al. 2015; Chen et al. 2017; Liu et al. 2017, 2018). Members of the homeotic MADS-box genes have been identified as key regulators controlling the orchestration of female reproductive organs during flower determination and development (Liljegren et al. 2000; Kater et al. 2006; Kaufmann et al. 2009; Hu et al. 2011). *AGAMOUS* (*AG*) is a key gene for plant sexual reproduction. *AG* is spatially restricted to the third and fourth whorls and functions redundantly with *APETALA2* (*AP2*), *LEUNIG* (*LUG*), *CURLY LEAF* (*CLF*), and *STERILE APETALA* (*SAP*). An *AG*-independent carpel development pathway has been identified (Bowman et al. 1989; Ito et al. 2007). Two redundant genes, *SHATTERPROOF1* (*SHP1*) and *SHP2*, are closely related to *AG* and specify valve margin identity (Liljegren et al. 2000). *HECATE* (*HEC*) cooperates with *SPATULA* (*SPT*) to regulate the female reproductive tract (Gremski et al. 2007). Functional exploration of *ETTIN* demonstrated that auxin involved in the polarity determinants of gynoecium (Nemhauser et al. 2000; Pagnussat et al. 2009). In tomato, the down-regulation of *ARF6* and *ARF8* targeted by *miR167* leads to defects in floral development and female sterility (Liu et al. 2014). A spontaneous frame-shift mutation (*fst*) in rice does not produce any activated embryos and endosperms with completely sterile females. Anatomical analysis showed that the abortion occurred in the sporophytic tissues including the integuments, fertilized pre-embryos, and endosperms (Lee et al. 2013). *Arabidopsis* YABBY and KANADI genes mutation causes amorphous or arrested integument growth (Eshed et al. 2001; McAbee et al. 2006). Examination of complex pistil structures is expected to provide information on their morphological development and gene regulatory networks.

Megasporocytes are derived from the differentiation of hypodermal cells in the ovule primordium. The sporocyte subsequently undergoes meiosis, giving rise to megaspores (Scott et al. 2004). A defect in any of these processes leads to the occurrence of plant sterility. Many important genes that play vital roles in ovule development have been identified. *SPOROCYTELESS/NOZZLE* (*SPL/NZZ*) of *Arabidopsis* is vital for the differentiation of megasporocytes and has complex regulatory mechanisms for sporogenesis (Ito et al. 2004; Wei et al. 2015). The *WUSCHEL* (*WUS*) homeobox gene facilitates the coordination of behaviors of different cell populations during ovule development (Groß-Hardt et al. 2002). In *Arabidopsis* female-sterile mutant, *aintegumenta* (*ant*), integuments were not observed and megasporogenesis was blocked at the tetrad stage (Elliott et al. 1996; Klucher et al. 1996). In *sterile apetala* (*sap*) mutants of *Arabidopsis*, megasporogenesis is arrested in ovules during meiotic division, with the tetrad and embryo sacs being entirely absent (Byzova et al. 1999).

The size and shape characteristics of mature plant organs vary among species and determine plant yield and biomass. The growth of plant organs is determined by cell proliferation and cell expansion (Sugimoto-Shirasu and Roberts 2003). These two processes are integrated. Subtle signals regulate the specific spatial and temporal patterns in organs to control their final size. Genetic and molecular mechanisms should be elucidated because they are vital for plant organ development. Certain factors regulating cell proliferation have been identified, including *AUXIN-REGULATED GENE INVOLVED IN ORGAN SIZE* (*ARGOS*), *AINTEGUMENTA* (*ANT*), *CINCINNATA* (*CIN*), *GROWTH-REGULATING FACTORS* (*GRFs*), *GRF-INTERACTING FACTORS* (*GIFs*), and *KLUH/CYP78A5* (Krizek 1999; Hu et al. 2003; Kim et al. 2003; Nath et al. 2003; Kim and Kende 2004; Anastasiou et al. 2007). *ROTUNDIFOLIA3* (*ROT3*), *ARGOS-LIKE* (*ARL*), *BIGPETAL* (*BPE*), *ROOT PHOTOTROPISM2* (*RPT2a*), *SMALL AUXIN UP RNA* (*SAUR*), *MEDIATOR25/PHYTOCHROME AND FLOWERING TIME 1* (*MED25/PFT1*), and *KUODA1* (*KUA1*) (Kim et al. 1998; Hu et al. 2006; Szécsi et al. 2006; Lee et al. 2011; Spartz et al. 2012; Xu and Li 2012; Lu et al. 2014) were identified controlling organ growth by regulating cell expansion. In *Arabidopsis*, the ubiquitin receptor *DA1* was found to regulate organ size by repressing cell proliferation (Li et al. 2008). Further, the mutant of *STERILE APETALA* (*SAP*)/SUPPRESSOR OF DA1 (SOD3) was found to suppress the *da1-1* phenotype. The biological function of *SAP* in controlling organ size by regulating cell proliferation was demonstrated by its interaction with KIX8/9 and PPDs (Wang et al. 2016; Li et al. 2018).

Ethyl methanesulfonate (EMS) is widely used to construct artificial mutant libraries because it is easy to handle and induces mutations at a high frequency (Serrat et al. 2014). Numerous EMS-induced mutant populations have been created in *Brassica*, with many important genes being identified. In oilseed rape EMS-induced mutant populations, *FAE1* was identified controlling erucic acid synthesis in the seed, as well as major genes involved in the sinapine biosynthesis pathway (Wang et al. 2008; Harloff et al. 2012). The *dyad* mutant of *Arabidopsis* was screened from EMS-mutagenized M_2 plants to identify female-sterile mutants (Siddiqi et al. 2000). It was mapped at the lower end of chromosome

5 with PCR-based simple sequence length polymorphism (SSLP) markers and F_2 populations. A maize *rotten ear* (*rte*) mutant that shows distinct defects in vegetative and reproductive development was identified in a series of EMS-mutagenized populations (Chatterjee et al. 2014). Positional cloning revealed that *rte* encodes a boron efflux transporter BOR1. Histology and microscopy observations between *rte* and wild-type plants revealed the structural importance of boron in the formation of reproductive organs. Mutants exhibiting sterility traits identified in EMS-mutagenized populations provide an excellent opportunity to explore the growth and development of plant reproductive organs. EMS mutagenesis usually causes random single-point G/C-to-A/T transitions (Sikora et al. 2011). It supports competent survival rates and forward and reverse genetic analyses.

Chinese cabbage is widely cultivated in East Asia. In the present study, a female-sterile mutant (*fsm*) was obtained from the Chinese cabbage DH line 'FT' in the process of inducing mutations with EMS (Huang et al. 2017). Simple sequence repeats (SSR) and insertion/deletion (Indels) markers were used to build a high-density genetic linkage map. Whole-genome re-sequencing was performed to detect variations in the target mapping region. A single-nucleotide polymorphism (SNP) that prematurely terminates amino acid coding in *BraA04001030* was confirmed. Therefore, *BraA04001030* was presumed as a candidate gene for *fsm*. This study facilitates further mutant gene cloning of *fsm* and contributes toward elucidating the molecular mechanisms underlying female sterility in Chinese cabbage.

Materials and methods

Plant materials

A doubled haploid (DH) line of Chinese cabbage, 'FT,' was used as the wild type for isolated microspore culture and ethyl methanesulfonate (EMS) mutagenesis. A female-sterile mutant (*fsm*) was identified from the populations. Cabbage Sprouts (*Brassica campestris* ssp. *chinensis* L.) DH line '701,' a material with distant relationship with Chinese cabbage, was used as the female parent to construct the segregating population.

Stigma surface observations by scanning electron microscopy (SEM)

Buds of 'FT' and *fsm* were randomly selected for self-pollination during flower opening. The pollinated stigmata were collected after 4 h. Samples were fixed in 2% glutaraldehyde at 4 °C overnight and then dehydrated with a graded ethanol dilution series (soak the sample in 50% alcohol solution, 75% alcohol solution, and 90% alcohol solution for about 5 min). Then, the samples were mounted on stubs and sputter-coated with gold. All samples were observed under a scanning electron microscope (Hitachi TM3030; Hitachi Ltd., Chiyoda, Tokyo, Japan).

Fluorescence staining of pollen tubes

Aniline blue staining was used to visualize the pollen tube growing within the pistil as described previously but with modifications (Chen et al. 2007). The day before flowering, stamens were removed from the bud. At the flower-opening stage, the pistils of the 'FT' and *fsm* flowers were self-pollinated. Pistils were collected 4 h after pollination and fixed in FAA solution (50% ethanol, 5% acetic acid, and 3.7% formaldehyde) at 4 °C overnight. They were then rinsed three times with distilled water and softened with 8 M NaOH for 12 h. Then, they were rinsed three times in 0.1 M K_3PO_4 (pH 8.0) and stained in 0.05% (w/v) aniline blue solution for 12 h in the dark. The pistils were observed and photographed under a fluorescence microscope (Axio Observer A1; Carl Zeiss AG, Oberkochen, Germany).

Construction of the mapping population

Classic map-based cloning methods were used to locate mutant genes. '701' was the designated female parent, and *fsm* was the male parent to construct the segregating population. The F_1 plants were self-pollinated, and F_2 plants with the mutant phenotype were used for linkage analysis and gene mapping. Plants were selected by visual examination for female sterility or fertility at flowering. The parental lines and the F_2 mapping population were grown in 2015 at the greenhouse of Shenyang Agriculture University, Liaoning Sheng, China.

DNA extraction, marker development, and PCR amplification

For the parents and F_2, total genomic DNA was extracted from fresh leaves using a modified version of the cetyltrimethylammonium bromide (CTAB) method and stored at − 30 °C. Polymerase chain reactions (PCR) were performed using a final reaction mixture volume of 10 µL. The PCR products were separated on 5% denaturing polyacrylamide gels at 220 V for 1.5 h and then subjected to silver staining.

A total of 749 SSR markers were used to identify polymorphisms between the two parents. They were obtained from the *Brassica rapa* Genome Sequencing Project (BrGSP) and were well distributed on ten linkage groups of the *Brassica* A genome. It was confirmed that the markers were closely linked to the *fsm* gene. Thus, new markers were designed in Primer Premier V. 5.0 (PREMIER Biosoft International, Palo Alto, CA, USA) based on the reference

genome sequence in the BRAD database (http://brassicadb.org/brad/). Newly developed SSR and Indel primers were synthesized by GENEWIZ, Inc., Tianjin, China.

Linkage analysis and genetic map construction

Tightly linked markers were first identified by screening 300 F_2 mapping populations. Larger F_2 populations and increasingly closely linked markers distributed on both sides of the mutant gene were subsequently obtained. A genetic linkage map between the molecular markers and the mutant gene was constructed according to the recombination frequencies of the polymorphic markers with MapMaker V. 3.0 (Whitehead Institute, Cambridge, MA, USA) (Lander et al. 1987). Map distances (centimorgans; cM) were calculated with the mapping function of Kosambi (1943).

Variation detection by whole-genome re-sequencing

Total genomic DNA was extracted from 'FT' and *fsm* as described in the previous section. The purity and quality were validated with Qubit and NanoDrop ND-1000 (NanoDrop Technologies LLC, Wilmington, DE, USA). Next, DNA-seq libraries were generated with a TruSeq Library Construction Kit (Illumina, Inc., San Diego, CA, USA). DNA samples were broken into 350-bp fragments by Covaris sonication. The fragments were blunt end-repaired, A-tailed, and ligated with full-length adapters for PCR amplification. The PCR products were purified (Agencourt AMPure XP; Beckman Coulter Inc., Brea, CA, USA) and sequenced on an Illumina HiSeq 2500 (Illumina, Inc., San Diego, CA, USA). The *Brassica rapa* reference genome was downloaded from the BRAD database. After quality control, clean data from two samples were aligned to the reference genome with Burrows-Wheeler Aligner (BWA) software (parameter: mem –t 4 –t 32 -M). Repetitive sequences were removed using SAMTOOLS (parameter: rmdup). SNP detection and annotation were performed with SAMTOOLS (parameter: mpileup –m 2 –F 0.002 –d 1000) and ANNOVAR, respectively.

Candidate gene prediction

To screen for candidate *fsm*, all annotations in the target region were identified in the *Brassica* database. Primers were designed to amplify the candidate genes according to the sequence information available in the *Brassica* database. The PCR amplification products were purified, cloned into the pGEM®-T Easy Vector (Promega, Madison, WI, USA), and transformed into the TOP10 competent cells (CWBIO, Beijing, China). Xgal-IPTG was added to the medium, and positive clones were selected by the blue-white spot. Recombinant plasmids were sequenced by GENEWIZ, Inc. (Tianjin, China). Multiple sequence alignments were performed in DNAMAN V. 6.0 (Lynnon LLC, San Ramon, CA, USA).

Quantitative real-time PCR (qRT-PCR) validation

Total RNA was extracted from buds and pistil of 'FT' and *fsm* using TRIzol reagent (Invitrogen, Carlsbad, CA, USA). The cDNA was synthesized using oligo (dT) primers and a FastQuant First-Strand cDNA Synthesis Kit (Tiangen, Beijing, China). The primer pair for the candidate gene *BraA04001030* (F: 5′-ACGCTACTGGGTCGGACTTTT-3′; R: 5′-ATAACAGCTTCTGGATCGGTGAG-3′) was used for qRT-PCR. *Actin* was used as an internal control (Huang et al. 2017). The reaction system was carried out with Real PreMix Plus (SYBR Green) on a Bio-Rad IQ5 real-time PCR detection system (Bio-Rad Laboratories, Hercules, CA, USA). The final reaction mixture volume was 20 μL, and the following program was run: pre-incubation at 95 °C for 5 min; 45 cycles of 95 °C for 30 s; 60 °C for 30 s; 72 °C for 15 s; and a final extension step of 72 °C for 30 min. Each cDNA sample was prepared in three biological replicates. The relative expression was calculated using the $2^{-\Delta\Delta Ct}$ method (Livak and Schmittgen 2001) and analyzed in Bio-Rad IQ5 Manager (Bio-Rad Laboratories, Hercules, CA, USA).

Results

Characterization of the *fsm* mutant

The morphological traits of the floral organs in *fsm* exhibited clear variation in the sepals, petals, stamens, and ovary (Fig. 1a–g). The ovaries of *fsm* were short and thin (Fig. 1g), and the seed pods failed to expand, even after artificial pollination. When crossed as a female, *fsm* was completely abortive, but it was fertile as a pollen donor. The organ size of leaves and flowers was noticeably smaller. The leaves of *fsm* were comparatively smaller than those of 'FT' at the seedling stage, and also the leafy heads (Fig. 1h, i). In a previous study, we demonstrated that the female abortion of *fsm* was caused by the abnormal development of the ovules (Huang et al. 2017). Genetic investigation showed that *fsm* was controlled by a single recessive nuclear gene.

Stigma observations

Female sterility of plants is mainly attributed to imperfect ovary structure or the dysfunction of embryo sac and female gametes. During the flowering day, the ovaries of *fsm* were wizened and failed to elongate, even under artificial pollination. To investigate whether female sterility

Fig. 1 Floral organ morphology of 'FT' and *fsm*. **a** Inflorescences of wild-type 'FT' (left) and mutant *fsm* (right); **b** single flower of 'FT.' **c** single flower of *fsm*. **d** sepals of 'FT' (left) and *fsm* (right); **e** petals of 'FT' (left) and *fsm* (right); **f** stamens of 'FT' (left) and *fsm* (right); **g** pistils of 'FT' (left) and *fsm* (right); **h** 'FT' (left) and *fsm* (right) at the seedling stage; and **i** leafy heads of 'FT' (left) and *fsm* (right). Scale bar: 1 mm

occurs during pollen–pistil interaction, we evaluated the pollen tube growth and papillar cell viability.

At the flower-opening stage, the papillae of 'FT' resembled normal rounded bilobed domes (Fig. 2a). The carpel apex was incompletely healed and left a groove or notch in the middle of the *fsm* stigma. The area covered by stigma mastoid cells was flat in *fsm* (Fig. 2b). The papillar cells of *fsm* were abnormally elongated. The papillar cells were oblate and large compared to those of 'FT' (Fig. 2c, d). Four hours after pollination, the pollen grains adhered to the stigmata of both 'FT' and *fsm*. They then hydrated and germinated on the papillar cells. Pollen tubes extended and penetrated the papillar cells (Fig. 2e, f). However, there were relatively fewer pollen grains adhering to the papillae in *fsm*. Although there were some morphological changes in the stigma cells, the function of the hydrated pollen grains was normal.

Pollen tube development

From the results of the pollen tube aniline blue staining of the pistil, after pollination, the pollen tube of the style in female-sterile mutant *fsm* was normal, and the sperm cells could penetrate the stigma and style (Fig. 2g, i). A more detailed observation revealed that the pollen tube also developed normally in the stalk portion of the ovule (Fig. 2j).

Preliminary mapping of the *fsm* gene

A map-based cloning strategy was adopted to isolate the mutant gene of *fsm*. A total of 176 pairs of SSR markers were uniformly distributed among ten linkage groups of the *Brassica* A genome and were used to detect polymorphisms between *fsm* and '701.' Of these, 67 markers exhibited polymorphism. Thirty homozygous recessive F_2 individuals

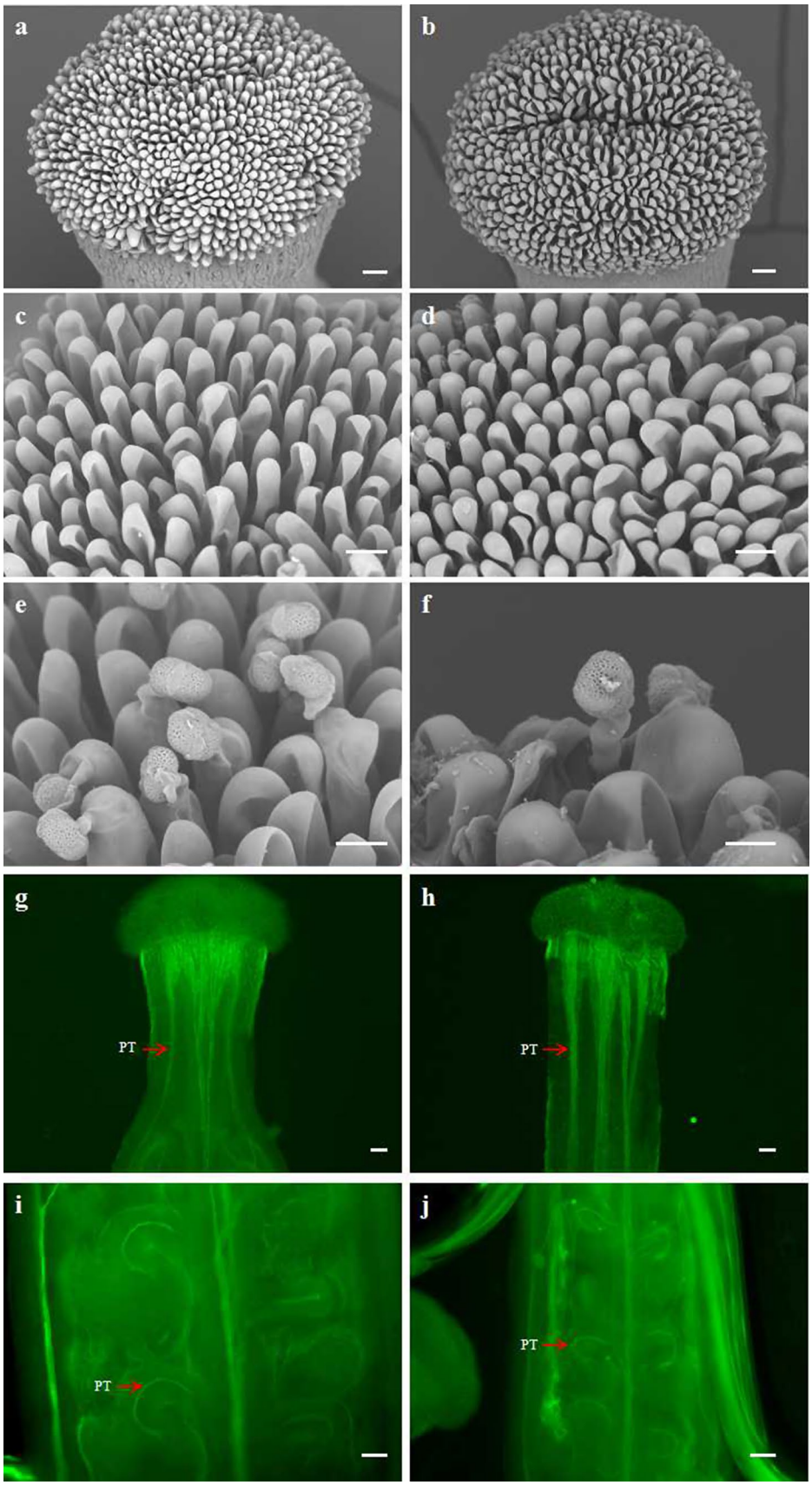

Fig. 2 Morphological observations of papillae under a scanning electron microscope (SEM) and aniline blue staining of pollen tube germination. **a** Papillae of 'FT'; **b** papillae of *fsm*; **c** phenotype of unpollinated papillar cell of 'FT'; **d** unpollinated papillar cell of *fsm*; **e** at 4 h after pollination, pollen tubes (Pt) emerged and penetrated 'FT' papillar cells; **f** At 4 h after pollination, pollen tubes (Pt) emerged and penetrate *fsm* papillae cells; **g** and staining of pollen tubes in the style of 'FT.' **h** Staining of pollen tubes in the style of *fsm*. **i** Pollen tubes penetrated embryo sacs in 'FT.' **j** Pollen tubes penetrated the embryo sacs in *fsm*. PT pollen tubes. Red arrows indicate pollen tubes. Scale bar: 20 μm

were selected to determine whether they were linked with the mutant loci. SSR marker cnu-m439a on chromosome A04 was linked to the target gene. It was used for screening in other homozygous recessive F_2 individuals for linkage analysis and gene mapping. The linkage analysis indicated that cnu-m439a was linked to *fsm* at a genetic distance of 1.16 cM (Fig. 3a).

Markers near cnu-m439a on chromosome A04 were developed for polymorphism detection and linkage analysis. The polymorphic molecular marker SSR-R39 was identified on the other side of the target locus. Its recombinants differed from cnu-m439a. The new markers SSR-g37, SSR-g17, SSR-R82, and SSR-g7 were located between cnu-m439a and SSR-R39 and were linked to the mutant loci (Fig. 3b, Table S1). Statistical analyses of the recombinants of these markers were conducted for linkage analysis and gene mapping. The results indicated that SSR-R39, SSR-g37, and SSR-g17 were located on the opposite side of *fsm* relative to SSR-R82, SSR-g7, and cnu-m439a. Recombination frequency data demonstrated that SSR-R82 and SSR-g17 were tightly linked to the mutant locus at genetic distances of 0.08 cM and 0.11 cM, respectively (Fig. 3a).

Fine mapping of *fsm* gene

New SSR and Indel markers were developed in the interval between SSR-R82 and SSR-g17 to map the mutant gene of *fsm* more precisely. SSR-g13, Indel-I2, and Indel-I7 exhibited polymorphisms and were tightly linked to *fsm* (Table S1). According to the number of recombinants, the target locus was between Indel-I2 and Indel-I7 at genetic distances of 0.05 cM and 0.06 cM, respectively (Fig. 3b). Therefore, the mutant gene was located in a 0.11-cM region on the A04 linkage group (Fig. 3c). When the genetic map was aligned to the *B. rapa* genome, it was found that the physical distance between Indel-I2 and Indel-I7 was 1376.69 kb and there were 107 genes in the target region (Fig. 3c, Table S2).

In traditional map-based cloning, molecular marker linkage analysis is based on the recombination rate between the marker and the target locus. Further increases of the mapped population failed to reveal more linkage markers to narrow the positioning interval. Next, whole-genome re-sequencing was conducted to detect variations between 'FT' and *fsm*. After filtering, sequencing quality was established. It was found that sample data volume was adequate, GC distribution was normal, and the database was successfully sequenced. Exonic, homozygous, and non-synonymously encoded mutation sites in the *fsm* were filtered out of the mutation sites detected by genomic re-sequencing.

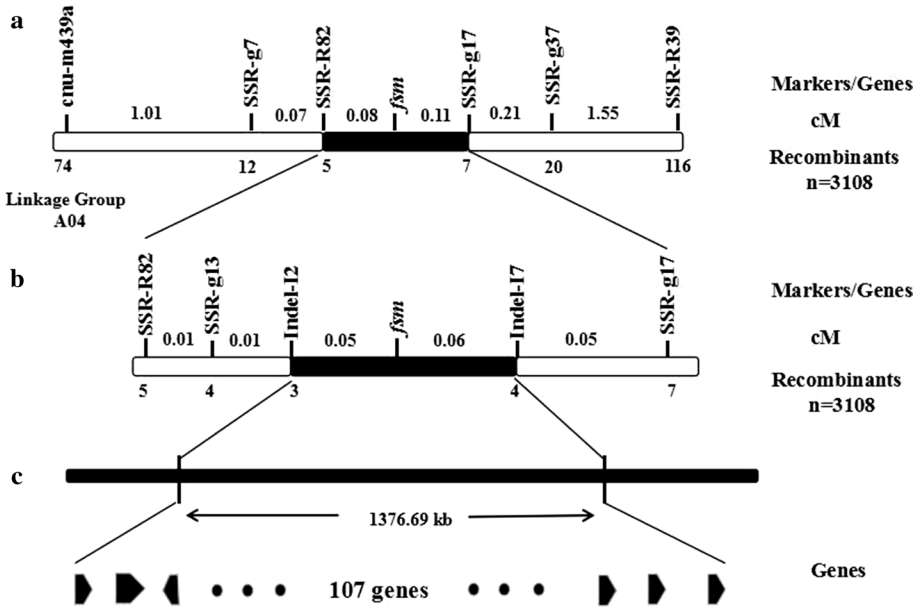

Fig. 3 Genetic and physical maps of the *fsm* gene and candidate gene analysis. **a** Linkage map of chromosome 4 constructed using 3108 sterile F_2 plants. The *fsm* gene was mapped to the region between SSR-R82 and SSR-g17. Numbers are genetic distances between adjacent markers; **b** fine mapping of the *fsm* gene. The *fsm* gene was restricted to a region between Indel-I2 and Indel-I7. The number of recombinants between the markers and *fsm* is indicated under the linkage map. Numbers are genetic distances in centimorgans (cM) between adjacent markers; **c** candidate region of the *fsm* locus annotated in the *Brassica* database. The *fsm* gene was narrowed down to a 1376-kb region containing 107 predicted genes. Detailed information on these genes is presented in Table S2

Candidate gene prediction

In the final mapping region between Indel-I2 and Indel-I7, 12 possible SNPs exist in *fsm* and were distributed on six genes (Table S3). Corresponding primers were designed to verify the sequence based on the locations of the 12 SNP sites. Sequencing alignment results confirmed that a single-nucleotide C-to-A (TCG/TAG) transition occurred in *BraA04001030*, causing the premature occurrence of a termination codon (Fig. 4b). Four pairs of primers were designed along the full length of *BraA04001030* to sequence the gene in *fsm* and 'FT.' Alignment analysis showed that only one single-nucleotide polymorphism (SNP) was found in *fsm*. It was consistent with the re-sequencing results. Genotype analysis of seven recombinants between the two most closely linked markers indicated that the female-sterile phenotype cosegregated with this SNP (Fig. S1). *BraA04001030* encodes a homologue of the *STERILE APETALA* (*SAP*) transcriptional regulator. In *Arabidopsis thaliana*, *SAP* regulates flower and ovule development (Byzova et al. 1999). Therefore, we selected *BraA04001030* as the most likely candidate gene for *fsm*.

The genomic sequence of *BraA04001030* is 1131 bp in length and has only one exon, which encodes a protein of 376 amino acid residues. The SNP (C-to-A) was located on the of 599th base and caused the termination of amino acid coding at the 200th residue (S → U) in *BraA04001030* of the *fsm* mutant (Fig. 4b). The amino acid sequence alignment showed a high similarity (75.00%) with *AtSAP* (*AT5G35770*). Proteins that share significant homology with *SAP* are found in *Brassica* and other species. A phylogenetic tree was constructed showing the kinship between these species (Fig. S2).

Analysis of gene expression

The expression levels of *BraA04001030* in *fsm* and 'FT' were examined by qRT-PCR. Gene expression levels in the inflorescence and pistils of *fsm* resembled those of the wild type (Fig. 5). The single-nucleotide polymorphism (SNP) that occurs in *BraA04001030* did not cause differences in expression between 'FT' and *fsm*.

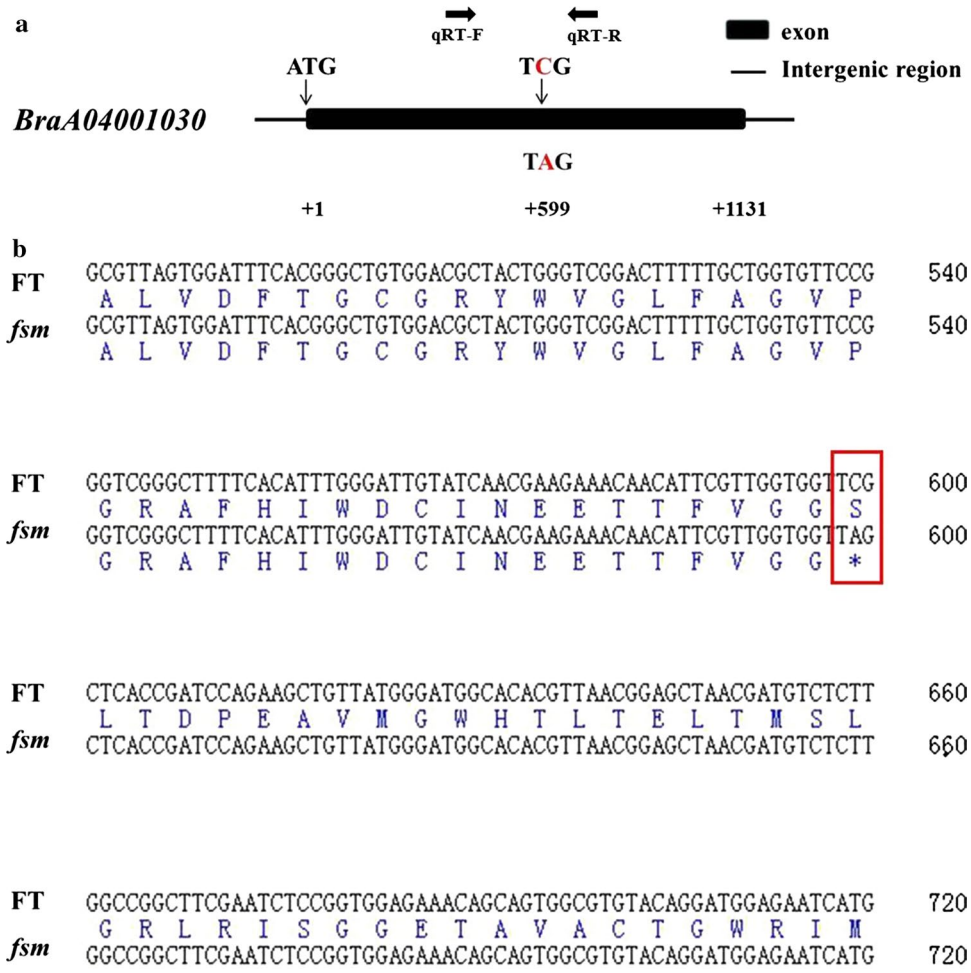

Fig. 4 Gene structure and alignment analysis of encoded amino acid sequences between 'FT' and *fsm*. **a** Gene structure of *BraA04001030* and the site of SNP. The arrows indicate the primers of qRT-PCR; **b** alignment of amino acid sequences between 'FT' and *fsm*. Red rectangle: position where encoded amino acid was prematurely terminated

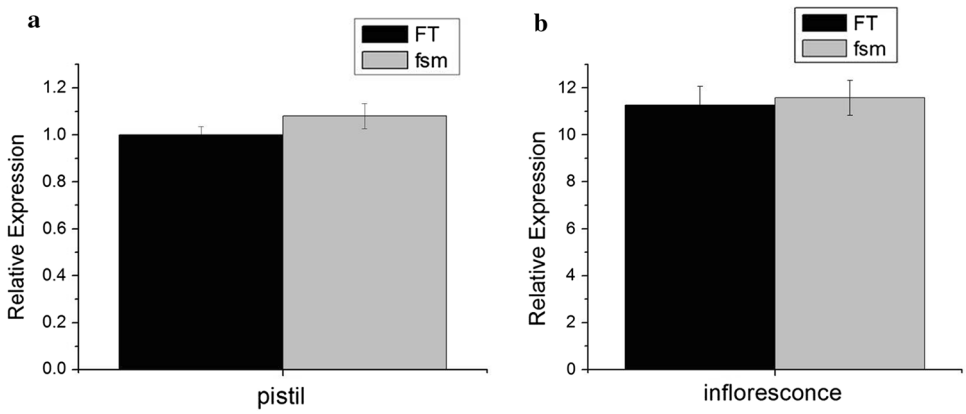

Fig. 5 Expression analysis of *BraA04001030* in 'FT' and *fsm* by qRT-PCR. **a** Pistil; **b** inflorescence

Discussion

The female organs of plants are highly complex. The use of female-sterile mutants could provide more insights into the mechanisms regulating flower development (Tedder et al. 2015). The female-sterile mutant (*fsm*) of Chinese cabbage is ideal for studying ovary and ovule development. In the current study, we showed that the growth of stigma papillar cells and pollen tubes was normal in the mutant *fsm*, based on pistil aniline blue staining and stigma scanning. Combined with previous observations of morphological characteristics in *fsm* ovaries (Huang et al. 2017), we consider that the pistil pollination process in *fsm* was not affected, but that sterility may due to the production of megasporocytes or the mitosis of functional megaspores. We performed genetic mapping of the *fsm* gene using a large F_2 population and a number of closely linked markers. Furthermore, genomic re-sequencing was conducted to detect possible variations in the target region. As a result, *BraA04001030* was predicted as the candidate gene for *fsm*. The female-sterile mutant of Chinese cabbage could be used as a basis for studies exploring the development process and molecular regulation mechanisms of pistils and ovules in Chinese cabbage.

Identification of the variant site of the mutant could be used to elucidate the occurrence of the mutant phenotype at the molecular level. Genetic mapping demonstrated that the mutant gene of *fsm* was anchored between the two most tightly linked markers on chromosome A04, namely Indel-I2 and Indel-I7. There was still a large area in the positioning interval, and numerous genes remained. No other effective polymorphic markers were found in this interval, and the candidate gene of *fsm* could not be more accurately characterized. When the location information was aligned to the *B. rapa* genome, it was found that the target region was in the centromeric region of chromosome A04 (Cheng et al. 2013). The low recombination rate and high frequency of repetitive sequences were associated with this region (Cheng et al. 2002). The heterochromatin structure and domains near the centromeres are highly complex. Consequently, further candidate gene identification was hindered in this region. Therefore, it remains a substantial challenge to clone, sequence, and assemble the genomic components in this region. In this study, whole-genome re-sequencing between 'FT' and *fsm* was conducted to detect variation in the final positioning interval. PCR amplification and Sanger sequencing were used for SNP validation since they are the gold standards for this purpose (Kang et al. 2015). A single-nucleotide polymorphism (SNP) was identified inside *BraA04001030*. This gene is orthologous to *Arabidopsis thaliana STERILE APETALA* (*AtSAP*) and plays vital roles in the regulation of flower and ovule development (Byzova et al. 1999). The SNP in *BraA04001030* causes premature stop coding, which may alter *SAP*-encoded protein activity and significantly influence vital traits. The relative expression of *SAP* in 'FT' and *fsm* was equivalent. This observation was consistent with *SAP* expression levels determined for *Arabidopsis sod3-1* (Wang et al. 2016). Single-nucleotide variation in a given gene might not necessarily alter gene expression. The abnormal function of *SAP* in *fsm* was manifested mainly in amino acid coding.

The reduced-fertility mutant *sap* of *Arabidopsis* was identified in a transposable element system, and its phenotype resembled that of *ap2* (Byzova et al. 1999). The ovules of *ap2-1* appeared normal. The *sap* single mutant showed defects in megasporogenesis. The genetic interaction between *SAP* and *AP2* was analyzed. There was no embryo sac in the *sap*/*ap2-1* mutant, and megaspores within the dyad or tetrad were not observed. Analysis of the pattern of expression of *sap ap2* double mutants and *sap* or *ap2* single mutants revealed that both genes function synergistically in the inflorescence meristem but were not coregulated. Megasporogenesis abortion occurs earlier in *sap ap2* when compared to single mutant *sap*. Therefore, both genes complement each other during the initiation of megasporogenesis. In our previous and current studies, the infertility of *fsm* was confirmed by the abortion of the ovule, which has the same phenotype as the *SAP* mutant in *Arabidopsis*. *AGAMOUS* (*AG*) was restricted by

APETALA2 (*AP2*) to the inner two floral whorls (Drews et al. 1991). In *Arabidopsis thaliana*, the *sap ag-1* double mutant exhibit unique floral architecture and axillary flower bud features. The phenotype of the double mutant indicates that *SAP* genetically interacts with *AG* to maintain the identity of the floral meristem. In Chinese cabbage, *fsm* also exhibits multiple axillary flower buds and similar floral architecture with *sap*. It remains to determine whether *SAP* genetically interacts with *AG* and *AP2* during the flower development of Chinese cabbage.

In addition, the *fsm* mutant of Chinese cabbage exhibited variation in organ size. The leaves, inflorescence, and flower organs of *fsm* were smaller than those of the wild-type 'FT.' The phenotype was consistent with that of the *sap* mutant in *Arabidopsis* (Wang et al. 2016). It was confirmed that *SAP* promotes meristemoid cell proliferation in *Arabidopsis*. In *fsm*, the organ size variation may be limited by cell proliferation. In *Arabidopsis*, the ubiquitin receptor DA1 acts synergistically with the E3 ubiquitin ligases DA2 and *ENHANCER OF DA1* (*EOD1*)/*BIG BROTHER* to regulate cell proliferation and control organ growth (Xia et al. 2013). The ubiquitin pathway regulates plant organ size (Du et al. 2014). Protein sequencing shows that *SAP* participates as an F-box protein in the SKP1/Cullin/F-box (SCF) E3 ubiquitin ligase complex (Wang et al. 2016). SCFs repress signaling in several phytohormone pathways that regulate plant growth and development (Gray et al. 2001). Recently, it was reported that *SAP* targets *PEAPODs* (*PPDs*) and *KIX8/9* proteins for degradation for controlling organ size (Wang et al. 2016; Li et al. 2018). Chinese cabbage is an important leafy crop. Exploring the molecular mechanism underlying plant organ size is expected to provide an important resource for breeding. Identification of mutant genes might help explain mutant phenotypes at the molecular level.

The accessibility of information on the Chinese cabbage genome has greatly facilitated map-based cloning. This study is the first to identify *SAP* as the candidate gene for female sterility in Chinese cabbage. Detailed mapping of the genetic interaction networks will help elucidate the ontogeny. Further exploration is required to characterize the molecular mechanisms underlying organ size and female reproductive development in Chinese cabbage.

Author contribution statement HF, WJL, SNH, and ZYL conceived and designed the study. WJL and TXL, CT, YHW performed the experiments. WJL wrote the paper. WJL, SNH, and HF reviewed and edited the manuscript. All authors read and approved the manuscript.

Funding The research was supported by the National Natural Science Foundation of China (Grant No. 31672144).

References

Anastasiou E, Kenz S, Gerstung M, MacLean D, Timmer J, Fleck C, Lenhard M (2007) Control of plant organ size by *KLUH/CYP78A5*-dependent intercellular signaling. Dev Cell 13:843–856. https://doi.org/10.1016/j.devcel.2007.10.001

Bencivenga S, Colombo L, Masiero S (2011) Cross talk between the sporophyte and the megagametophyte during ovule development. Sex Plant Reprod 24:113–121. https://doi.org/10.1007/s00497-011-0162-3

Bowman JL, Smyth DR, Meyerowitz EM (1989) Genes directing flower development in *Arabidopsis*. Plant Cell 1:37–52. https://doi.org/10.1105/tpc.1.1.37

Byzova MV, Franken J, Aarts MG, de AlmeidaEngler J, Engler G, Mariani C, Van Lookeren Campaqne MM, Angenent GC (1999) *Arabidopsis STERILE AAPETALA*, a multifunctional gene regulating inflorescence, flower, and ovule development. Genes Dev 13:1002–1014. https://doi.org/10.1101/gad.13.8.1002

Cao L, Wang S, Venglat P, Zhao L, Cheng Y, Ye S, Qin Y, Datla R, Zhou Y, Wang H (2018) *Arabidopsis* ICK/KRP cyclin-dependent kinase inhibitors function to ensure the formation of one megaspore mother cell and one functional megaspore per ovule. PLoS Genet 14:e1007230. https://doi.org/10.1371/journal.pgen.1007230

Chatterjee M, Tabi Z, Galli M, Malcomber S, Buck A, Muszynski M, Gallavotti A (2014) The boron efflux transporter ROTTEN EAR is required for maize inflorescence development and fertility. Plant Cell 26:2962–2977. https://doi.org/10.1105/tpc.114.125963

Chen YH, Li HJ, Shi DQ, Yuan L, Liu J, Sreenivasan R, Baskar R, Grossniklaus U, Yang WC (2007) The central cell plays a critical role in pollen tube guidance in *Arabidopsis*. Plant Cell 19:3563–3577. https://doi.org/10.1105/tpc.107.053967

Chen L, Zhang J, Li H, Niu J, Xue H, Liu B, Wang Q, Luo X, Zhang F, Zhao D, Cao S (2017) Transcriptomic analysis reveals candidate genes for female sterility in pomegranate flowers. Front Plant Sci 8:1430. https://doi.org/10.3389/fpls.2017.01430

Cheng Z, Dong F, Langdon T, Ouyang S, Buell CR, Gu M, Blattner FR, Jiang J (2002) Functional rice centromeres are marked by a satellite repeat and a centromere-specific retrotransposon. Plant Cell 14:1691–1704. https://doi.org/10.1105/tpc.003079

Cheng F, Mandáková T, Wu J, Xie Q, Lysak MA, Wang X (2013) Deciphering the diploid ancestral genome of the Mesohexaploid *Brassica rapa*. Plant Cell 25:1541–1554. https://doi.org/10.1105/tpc.113.110486

Coen ES, Meyerowitz EM (1991) The war of the whorls: genetic interactions controlling flower development. Nature 353:31–37. https://doi.org/10.1038/353031a0

Drews GN, Bowman JL, Meyerowitz EM (1991) Negative regulation of the *Arabidopsis* homeotic gene *AGAMOUS* by the *APETALA2* product. Cell 65:991–1002. https://doi.org/10.1016/0092-8674(91)90551-9

Du L, Li N, Chen L, Xu Y, Li Y, Zhang Y, Li C, Li Y (2014) The ubiquitin receptor DA1 regulates seed and organ size by modulating the stability of the ubiquitin-specific protease UBP15/SOD2 in *Arabidopsis*. Plant Cell 26:665–677. https://doi.org/10.1105/tpc.114.122663

Elliott RC, Betzner AS, Huttner E, Oakes MP, Tucker WQ, Gerentes D, Pere P, Smyth DR (1996) *AINTEGUMENTA*, an *APETALA2*-like gene of *Arabidopsis* with pleiotropic roles in ovule development and floral organ growth. Plant Cell 8:155–168. https://doi.org/10.2307/3870261

Eshed Y, Baum SF, Perea JV, Bowman JL (2001) Establishment of polarity in lateral organs of plants. Curr Biol 11:1251–1260. https://doi.org/10.1016/S0960-9822(01)00392-X

Gray WM, Kepinski S, Rouse D, Leyser O, Estelle M (2001) Auxin regulates SCF^{TIR1}-dependent degradation of AUX/IAA proteins. Nature 414:271–276. https://doi.org/10.1038/35104500

Gremski K, Ditta G, Yanofsky MF (2007) The *HECATE* genes regulate female reproductive tract development in *Arabidopsis thaliana*. Development 134:3593–3601. https://doi.org/10.1016/j.jfluchem.2006.06.018

Groß-Hardt R, Lenhard M, Laux T (2002) *WUSCHEL* signaling functions in interregional communication during *Arabidopsis* ovule development. Genes Dev 16:1129–1138. https://doi.org/10.1101/gad.225202

Harloff HJ, Lemcke S, Mittasch J, Frolov A, Wu JG, Dreyer F, Leckband G, Junq C (2012) A mutation screening platform for rapeseed (*Brassica napus*, L.) and the detection of sinapine biosynthesis mutants. Theor Appl Genet 124:957–969. https://doi.org/10.1007/s00122-011-1760-z

Hu Y, Xie Q, Chua NH (2003) The *Arabidopsis* auxin-inducible gene *ARGOS* controls lateral organ size. Plant Cell 15:1951–1961. https://doi.org/10.1105/tpc.013557

Hu Y, Poh HM, Chua NH (2006) The *Arabidopsis ARGOS-LIKE* gene regulates cell expansion during organ growth. Plant J 47:1–9. https://doi.org/10.1111/j.1365-313X.2006.02750.x

Hu L, Liang W, Yin C, Cui X, Zong J, Wang X, Hu J, Zhang D (2011) Rice MADS3 regulates ROS homeostasis during late anther development. Plant Cell 23:515–533. https://doi.org/10.1105/tpc.110.074369

Huang SN, Liu ZY, Li CY, Yao RP, Li DY, Hou L, Li X, Liu WJ, Feng H (2017) Transcriptome analysis of a female-sterile mutant (*fsm*) in Chinese cabbage (*Brassica campestris* ssp. *pekinensis*). Front Plant Sci 8:546. https://doi.org/10.3389/fpls.2017.00546

Ito T, Wellmer F, Yu H, Das P, Ito N, Alves-ferreira M, Riechmann JL, Meyerowitz EM (2004) The homeotic protein AGAMOUS controls microsporogenesis by regulation of *SPOROCYTELESS*. Nature 430:356–360. https://doi.org/10.1038/nature02733

Ito T, Ng KH, Lim TS, Yu H, Meyerowitz EM (2007) The homeotic protein AGAMOUS controls late stamen development by regulating a jasmonate biosynthetic gene in *Arabidopsis*. Plant Cell 19:3516–3529. https://doi.org/10.1105/tpc.107.055467

Kang S, Kim BG, Han HH, Lee JH, Kim JE, Shim HS, Cho NH (2015) Targeted sequencing with enrichment PCR: a novel diagnostic method for the detection of EGFR mutations. Oncotarget 6:13742–13749. https://doi.org/10.18632/oncotarget.3807

Kater MM, Dreni L, Colombo L (2006) Functional conservation of MADS-box factors controlling floral organ identity in rice and *Arabidopsis*. J Exp Bot 57:3433. https://doi.org/10.1093/jxb/erl097

Kaufmann K, Muiño JM, Jauregui R, Airoldi CA, Smaczniak C, Krajewski P, Angenent GC (2009) Target genes of the MADS transcription factor SEPALLATA3: integration of developmental and hormonal pathways in the *Arabidopsis* flower. PLoS Biol 7:e1000090. https://doi.org/10.1371/journal.pbio.1000090

Kim JH, Kende H (2004) A transcriptional coactivator, AtGIF1, is involved in regulating leaf growth and morphology in *Arabidopsis*. Proc Natl Acad Sci USA 101:13374–13379. https://doi.org/10.1073/pnas.0405450101

Kim GT, Tsukaya H, Uchimiya H (1998) The ROTUNDIFOLIA3 gene of Arabidopsis thaliana encodes a new member of the cytochrome P-450 family that is required for the regulated polar elongation of leaf cells. Genes Dev 12:2381–2391. https://doi.org/10.1101/gad.12.15.2381

Kim JH, Choi D, Kende H (2003) The AtGRF family of putative transcription factors is involved in leaf and cotyledon growth in *Arabidopsis*. Plant J 36:94–104. https://doi.org/10.1046/j.1365-313X.2003.01862.x

Klucher KM, Chow H, Reiser L, Fischer RL (1996) The *AINTEGUMENTA* gene of *Arabidopsis* required for ovule and female gametophyte development is related to the floral homeotic gene *APETALA2*. Plant Cell 8:137–153. https://doi.org/10.1105/tpc.8.2.137

Kosambi DD (1943) The estimation of map distances from recombination values. Ann Eugenics 12(1):172–175

Krizek BA (1999) Ectopic expression of *AINTEGUMENTA* in *Arabidopsis* plants results in increased growth of floral organs. Dev Genet 25:224–236. https://doi.org/10.1002/(SICI)1520-6408(1999)25:3%3c224:AID-DVG5%3e3.0.CO;2-Y

Kuusk S, Sohlberg JJ, Lonq JA, Fridborg I, Sundberg E (2002) *STY1* and *STY2* promote the formation of apical tissues during *Arabidopsis* gynoecium development. Development 129:4707–4717. https://doi.org/10.1007/s00429-002-0268-3

Lander ES, Green P, Abrahamson J, Barlow A, Daly MJ, Lincoln SE, Newberg LA (1987) MAPMAKER: an interactive computer package for constructing primary genetic linkage maps of experimental and natural populations. Genomics 1:174–181. https://doi.org/10.1016/j.ygeno.2008.12.003

Lee KH, Minami A, Marshall RS, Book AJ, Farmer LM, Walker JM, Vierstra RD (2011) The RPT2 subunit of the 26S proteasome directs complex assembly, histone dynamics, and gametophyte and sporophyte development in *Arabidopsis*. Plant Cell 23:4298–4317. https://doi.org/10.1105/tpc.111.089482

Lee DS, Chen LJ, Li CY, Liu Y, Tan XL, Lu BR, Li J, Gan SX, Kang SG, Suh HS, Zhu Y (2013) The B_{sister} MADS Gene *FST* determines ovule patterning and development of the zygotic embryo and endosperm. PLoS ONE 8:e58748. https://doi.org/10.1371/journal.pone.0058748

Li SC, Yang L, Deng QM, Wang SQ, Wu FQ, Li P (2006) Phenotypic characterization of a female sterile mutant in rice. J Integr Plant Biol 48:307–314. https://doi.org/10.1111/j.1744-7909.2006.00228.x

Li Y, Zheng L, Corke F, Smith C, Bevan MW (2008) Control of final seed and organ size by the *DA1* gene family in *Arabidopsis thaliana*. Genes Dev 22:1331–1336. https://doi.org/10.1101/gad.463608

Li N, Liu Z, Wang Z, Ru L, Gonzalez N, Baekelandt A, Pauwels L, Goossens A, Xu R, Zhu Z, Inzé D, Li Y (2018) *STERILE APETALA* modulates the stability of a repressor protein complex to control organ size in *Arabidopsis thaliana*. PLoS Genet 14:e1007218. https://doi.org/10.1371/journal.pgen.1007218

Liljegren SJ, Ditta GS, Eshed Y, Savidqe B, Bowman JL, Yanofsky MF (2000) SHATTERPROOF MADS-box genes control seed dispersal in *Arabidopsis*. Nature 404:766–770. https://doi.org/10.1038/35008089

Liu N, Wu S, Van Houten J, Wang Y, Ding B, Fei Z, Clarke TH, Reed JW, van der Knaap E (2014) Down-regulation of *AUXIN RESPONSE FACTORS 6* and *8* by microRNA 167 leads to floral development defects and female sterility in tomato. J Exp Bot 65:2507–2520. https://doi.org/10.1093/jxb/eru141

Liu H, Wu Y, Cao A, Mao B, Zhao B, Wang J (2017) Genome-wide analysis of DNA methylation during ovule development of female-sterile rice *fsv1*. G3 7:3621–3635. https://doi.org/10.1534/g3.117.300243

Liu S, Zhang Y, Feng Q, Qin L, Pan C, Lamin-Samu AT, Lu G (2018) Tomato AUXIN RESPONSE FACTOR 5 regulates fruit set and development via the mediation of auxin and gibberellin signaling. Sci Rep 8:2971. https://doi.org/10.1038/s41598-018-21315-y

Livak KJ, Schmittgen TD (2001) Analysis of relative gene expression data using real-time quantitative PCR and the 2(−Delta Delta C (T)) method. Methods 25:402–408. https://doi.org/10.1006/meth.2001.1262

Lu D, Wang T, Persson S, Mueller-Roeber B, Schippers JH (2014) Transcriptional control of ROS homeostasis by KUODA1 regulates cell expansion during leaf development. Nat Commun 5:3767. https://doi.org/10.1038/ncomms4767

McAbee JM, Hill TA, Skinner DJ, Izhaki A, Hauser BA, Meister RJ, Venuqopala Reddy G, Meyerowitz EM, Bowman JL, Gasser CS (2006) *ABERRANT TESTA SHAPE* encodes a KANADI family member, linking polarity determination to separation and growth of *Arabidopsis* ovule integuments. Plant J 46:522–531. https://doi.org/10.1111/j.1365-313X.2006.02717.x

Nath U, Crawford BC, Carpenter R, Coen E (2003) Genetic control of surface curvature. Science 299:1404–1407. https://doi.org/10.1126/science.1079354

Nemhauser JL, Feldman LJ, Zambryski PC (2000) Auxin and ETTIN in *Arabidopsis* gynoecium morphogenesis. Development 127:3877–3888. https://doi.org/10.1002/1097-0320(20000901)41:1%3c73:AID-CYTO10%3e3.0.CO;2-5

Pagnussat GC, Alandete-Saez M, Bowman JL, Sundaresan V (2009) Auxin-dependent patterning and gamete specification in the *Arabidopsis* female gametophyte. Science 324:1684–1689. https://doi.org/10.1126/science.1167324

Pinyopich A, Ditta GS, Savidge B, Liljegren SJ, Baumann E, Wisman E, Yanofsky MF (2003) Assessing the redundancy of MADS-box genes during carpel and ovule development. Nature 424:85–88. https://doi.org/10.1038/nature01741

Scott RJ, Spielman M, Dickinson HG (2004) Stamen structure and function. Plant Cell 16:S46–S60. https://doi.org/10.1016/j.laa.2009.09.016

Serrat X, Esteban R, Guibourt N, Moysset L, Nogués S, Lalanne E (2014) EMS mutagenesis in mature seed-derived rice calli as a new method for rapidly obtaining TILLING mutant populations. Plant Methods 10:5. https://doi.org/10.1186/1746-4811-10-5

Siddiqi I, Ganesh G, Grossniklaus U, Subbiah V (2000) The *dyad* gene is required for progression through female meiosis in *Arabidopsis*. Development 127:197–207. https://doi.org/10.1002/jcla.2062

Sikora P, Chawade A, Larsson M, Olsson J, Olsson O (2011) Mutagenesis as a tool in plant genetics, functional genomics, and breeding. Int J Plant Genomics 2011:314829. https://doi.org/10.1155/2011/314829

Singh SK, Kumar V, Srinivasan R, Ahuja PS, Bhat SR, Bhat SR, Sreenivasulu Y (2017) The *TRAF Mediated Gametogenesis Progression* (*TRAMGaP*) gene is required for megaspore mother cell specification and gametophyte development. Plant Physiol 175:1220–1237. https://doi.org/10.1104/pp.17.00275

Spartz AK, Lee SH, Wenger JP, Gonzalez N, Itoh H, Inzé D, Peer WA, Murphy AS, Overvoorde PJ, Gray WM (2012) The *SAUR19* subfamily of *SMALL AUXIN UP RNA* genes promote cell expansion. Plant J 70:978–990. https://doi.org/10.1111/j.1365-313X.2012.04946.x

Sugimoto-Shirasu K, Roberts K (2003) 'Big it up': endoreduplication and cell-size control in plants. Curr Opin Plant Biol 6:544–553. https://doi.org/10.1016/j.pbi.2003.09.009

Sundaresan V, Alandetesaez M (2010) Pattern formation in miniature: the female gametophyte of flowering plants. Development 137:179–189. https://doi.org/10.1242/dev.030346

Szécsi J, Joly C, Bordji K, Varaud E, Cock JM, Dumas C, Bendahmane M (2006) *BIGPETALp*, a *bHLH* transcription factor is involved in the control of *Arabidopsis* petal size. EMBO J 25:3912–3920. https://doi.org/10.1038/sj.emboj.7601270

Tedder A, Helling M, Pannell JR, Shimizu-Inatsugi R, Kawagoe T, Campen J, Sese J, Shimizu KK (2015) Female sterility associated with increased clonal propagation suggests a unique combination of androdioecy and asexual reproduction in populations of *Cardamine amara* (Brassicaceae). Ann Bot 15:763–776. https://doi.org/10.1093/aob/mcv006

Wang N, Wang Y, Tian F, King GJ, Zhang C, Long Y, Shi L, Meng J (2008) A functional genomics resource for *Brassica napus*: development of an EMS mutagenized population and discovery of *FAE1* point mutations by TILLING. New Phytol 180:751–765. https://doi.org/10.1111/j.1469-8137.2008.02619.x

Wang Z, Li N, Jiang S, Gonzalez N, Huang X, Wang Y, Inzé D, Li Y (2016) SCF^{SAP} controls organ size by targeting PPD proteins for degradation in *Arabidopsis thaliana*. Nat Commun 7:11192. https://doi.org/10.1038/ncomms11192

Wei B, Zhang J, Pang C, Yu H, Guo D, Jiang H, Ding M, Chen Z, Tao Q, Gu H, Qu LJ, Qin G (2015) The molecular mechanism of SPOROCYTELESS/NOZZLE in controlling *Arabidopsis* ovule development. Cell Res 25:121–134. https://doi.org/10.1038/cr.2014.145

Xia T, Li N, Dumenil J, Li J, Kamenski A, Bevan MW, Gao F, Li YH (2013) The ubiquitin receptor DA1 interacts with the E3 ubiquitin ligase DA2 to regulate seed and organ size in *Arabidopsis*. Plant Cell 25:3347–3359. https://doi.org/10.1105/tpc.113.115063

Xu R, Li Y (2012) The mediator complex subunit 8 regulates organ size in *Arabidopsis thaliana*. Plant Signal Behav 7:182–183. https://doi.org/10.4161/psb.18803

Yang L, Wu Y, Yu M, Mao B, Zhao B, Wang J (2016) Genome-wide transcriptome analysis of female-sterile rice ovule shed light on its abortive mechanism. Planta 244:1011–1028. https://doi.org/10.1007/s00425-016-2563-x

Zhou HC, Jin L, Li J, Wang XJ (2016) Altered callose deposition during embryo sac formation of multi-pistil mutant (*mp1*) in *Medicago sativa*. Genet Mol Res. https://doi.org/10.4238/gmr.15027968